

Research Proposal:
On the stability of elliptical periodic configurations of
the Three-Body Problem

Harry Kanyang Ying

June 2021

Abstract

This research is focused on the special case of the three-body problem with two primaries and one satellite. A theoretical model will be constructed with analytical solutions, and a computer simulation will be used based on this model. We will analyze the stability of such systems by making perturbations to the initial conditions of the system and simulating the movement of the bodies over time.

Contents

I	Introduction	4
1	Personal Interest	4
2	Literature Review	4
3	Methodology	4
4	Timeline	5
II	Aim	6
5	Research Question	6
6	Why Research Topic	6
III	Analysis of the problem	7
7	Analytical Solutions to Elliptical Lagrangian Points	7
7.1	Preliminary Analysis	7
7.1.1	Problem Setup	7
7.1.2	Change of Reference Frame	7
7.1.3	Specific Angular Momentum	10
7.1.4	Implications of Angular-Invariance	10
7.2	Equations of Motion	12
7.2.1	Collinear Cases	12
7.2.2	Non-collinear Cases	15
8	Stability Analysis	16
8.1	General Analysis	16
8.2	Analysis on Stability of Non-collinear Circular Cases	17
8.3	Stability of Non-collinear cases through Simulation	19
8.3.1	Construction of the Model	19
8.3.2	Effect of Perturbations	20
IV	Conclusion	23
9	Solutions to the Problem	23
10	Stability of the Solutions	23

Works Cited	24
-------------	----

Appendix	25
----------	----

A Programs	25
------------	----

B Graphs	27
----------	----

Figures

1	The initial setup of the two primaries	7
2	The two reference frames	8
3	Orbit of L2	15
4	Comparison between results	19
5	Orbits under perturbations	20
6	Orbits with smaller deviations	20
7	Plots of position against time	21
8	Orbits under larger perturbations	27

Codes

1	Iterative program for stability analysis.	25
---	---	----

Part I

Introduction

1 Personal Interest

The case of a satellite or moon orbiting a planet in a solar system is very common in the actual universe. Moreover, the orbit of the earth around the sun is well known to be elliptical. Therefore, the Sun-Earth-Moon system could be seen as one of those, and this research would give us insight on the stability of our moon. Also, it could provide solutions of how to place satellite in a more general setting.

Even though our solar system seems stable, research has already shown that chaotic aspects do exist ([Sussman and Wisdom 433](#)). Our model is useful for examining the stability of our surrounding system, especially focusing on the moons and satellites.

2 Literature Review

The existence of analytical solutions to the general three-body problem has been proved as a power series ([Cruz 11](#)). However, it doesn't provide practical insights to the general solution, as the power series converges extremely slowly. Other research focus has been put on either mathematically-harmonic special cases ([Montgomery and Chenciner](#)) or cases of practical usages, like the restricted version of the three-body problem.

As for the restricted circular three-body problem, there are 3 equilibrium points with unstable stability found and 2 with limited stability. The stability of the elliptical one was also analyzed ([Broucke 275](#)). However, there is no evident research on the elliptical solution conditions of Lagrangian orbits.

3 Methodology

For this research, we will begin by building a theoretical model with classical and celestial mechanics. Then, we will simulate this model through an iterative method, since the differential equations in this model are probably impossible to solve directly. Then, we will change the parameters of the simulation, such as the mass of the moon, the radii of the orbits, and analyze the conditions for stability of such star-planet-moon systems.

Furthermore, we could possibly run the simulation with the parameters of our solar system (such as the Sun, the Earth and the Moon), and evaluate the stability of our system.

4 Timeline

Table 1: The planned timeline of the research project.

30-Apr	Do background research for the topic. Synthesize and finish writing the literature review part of the proposal.
15-May	Develop a theoretical model of the research question. This model may be used to power the computer simulation, or may be used to compare with the simulation results.
30-May	Program the simulation. Analyze the results, and do data evaluation.
10-Jun	Finish writing the proposal.
20-Jun	Prepare poster and presentation.

Part II

Aim

5 Research Question

The research question we have chosen is: How stable and resilient are the elliptical periodic orbits in three-body problem?

Our topic of interest is to look at the stability of orbits and will focus on kinematics, dynamics and astrophysics.

6 Why Research Topic

The three-body problem and its potential solution is of particular interests both in the early modern period and contemporary context, for that most of the realistic celestial problems can be reduced into one type of the three-body problems. Those include natural star systems, which correspond to the general case of the three-body problem; satellite-star case, which is of the elliptical, restricted form; and the Sun-Earth-Satellite case, which fall into the circular, restricted category.

Stability of the proposed orbit is researched intensively and interested by many, because of the nature that errors and imprecision exist in applications, and to maintain an orbit, stability has to be analyzed to see if the orbit or the point is error-tolerant. In addition to that, stability also enables long-term prediction without going under meticulous calculations and precised initial values, which are common in astrophysics and astronomy.

Part III

Analysis of the problem

7 Analytical Solutions to Elliptical Lagrangian Points

We first set up the problem in a convenient way mathematically to our later steps. Then, a few key conditions are derived from the angular-invariance condition. Those conditions are analyzed, using which the solutions are split into two parts: collinear and triangular. Finally, the equations of motion are separately analyzed and solved.

7.1 Preliminary Analysis

7.1.1 Problem Setup

There are two primaries with masses M_1 and M_2 as they are in the traditional two-body problem. For the sake of an easier analysis, we take O in an inertial reference frame K whose x axis is in the direction of the line connecting the two primaries. In this frame K , we define the displacements of these two primaries as \mathbf{r}_1 and \mathbf{r}_2 respectively. We then define the third object with mass $m \ll M_2$. The displacement of the satellite under the gravitational forces the satellite exerts on both primaries are neglected. The motion of the primaries from Kepler's laws of planetary motions can be used.

Without loss of generality, we let angular velocity $\boldsymbol{\Omega}$ pointing in the positive z direction, i.e. counterclockwise and that $\omega = |\boldsymbol{\Omega}| > 0$. Furthermore, when $t = 0$, we take two primaries to be at their own periastrons with M_1 on the negative x axis (i.e. left-hand side) and M_2 on the positive x axis (i.e. right-hand side).

In our proposal, we are only interested in solutions that are periodic and "angular-invariant". By "angular-invariant", we mean that the angle that \mathbf{r}_3 makes with \mathbf{r}_1 is invariant throughout the motion. We call these solutions "elliptical Lagrangian" as they are able to reduce into circular Lagrange points.

7.1.2 Change of Reference Frame

It is often convenient to analyze the situation under a rotational reference frame in order to reduce the vector nature of the problem into pure scalar analysis. Using our knowledge on two-body planar motion, we know that $\mathbf{r}_1, \mathbf{r}_2, \mathbf{r}_{21} = \mathbf{r}_2 - \mathbf{r}_1$ are vectors parallel to each other, and that O is on the line through M_1 and M_2 .

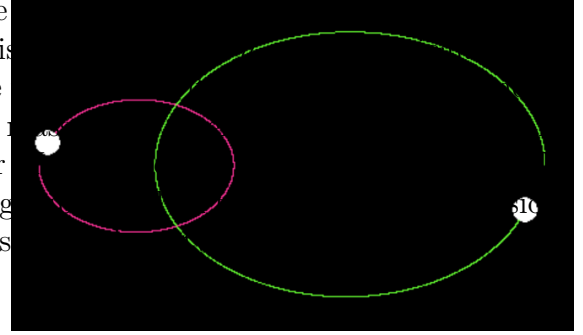


Figure 1: The initial setup of the two primaries.

We define our rotational reference frame K' such that at any time, \mathbf{r}_{21} observed from K' is on the x axis of the K' . The center of rotation of K' is at the barycenter of primaries, and the angle K' rotates at any time $\theta(t)$ is the angle that M_2O makes with the positive x axis of K . We use primed notation to denote the quantities relative to our rotational reference frame K' . For example, \mathbf{r}'_{21} means the \mathbf{r}_{21} perceived under K' . Finally, notice that under our definition, $\theta(0) = 0$.

Using our definition of the reference frame, we can describe the relation between K and K' using

$$\mathbf{r}'(t) = R(t) \cdot \mathbf{r}(t)$$

where

$$R(t) = \begin{bmatrix} \cos(-\theta(t)) & -\sin(-\theta(t)) \\ \sin(-\theta(t)) & \cos(-\theta(t)) \end{bmatrix}$$

The first thing to notice here is that $R(t)$ does the work of mere rotation. Therefore, $|\mathbf{r}(t)| = |\mathbf{r}'(t)| = r(t) = r'(t)$ for any $\mathbf{r}(t)$.

Now, we derive a few lemmas used later in establishing the acceleration between two reference frames:

$$\frac{dR}{dt} \cdot R^{-1} = -\omega \cdot \begin{bmatrix} 0 & -1 \\ 1 & 0 \end{bmatrix}$$

We also have

$$\begin{aligned} \frac{d}{dt}(RR^{-1}) &= \frac{d}{dt}I \\ \frac{dR}{dt} \cdot R^{-1} + \frac{dR^{-1}}{dt} \cdot R &= 0 \\ \frac{dR}{dt} \cdot R^{-1} &= -\frac{dR^{-1}}{dt} \cdot R \end{aligned}$$

Therefore, we also have following two equations for any vector \mathbf{p} ,

$$\begin{aligned} \left(\frac{dR}{dt} \cdot R^{-1} \right) \cdot \mathbf{p} &= -\boldsymbol{\Omega} \times \mathbf{p} \\ \left(\frac{dR^{-1}}{dt} \cdot R \right) \cdot \mathbf{p} &= \boldsymbol{\Omega} \times \mathbf{p} \end{aligned}$$

Using the above lemmas, we then obtain the relation between acceleration in K and that in K' ,

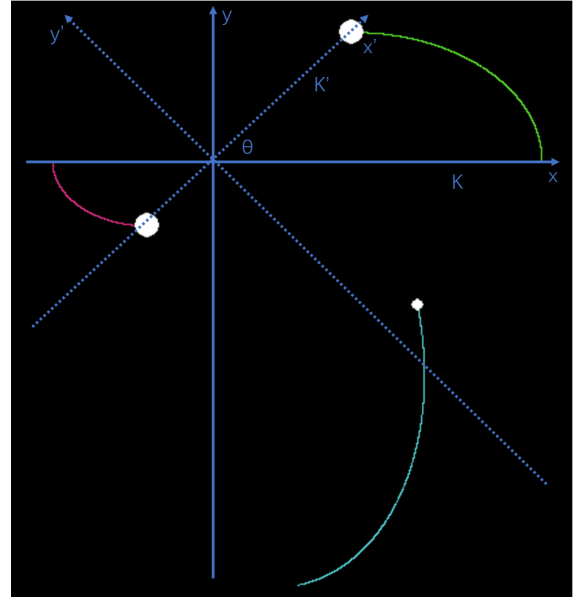


Figure 2: The two reference frames for a sample situation.

$$\begin{aligned}
\frac{d\mathbf{r}'}{dt} &= \frac{dR}{dt} \cdot \mathbf{r} + R \cdot \frac{d\mathbf{r}}{dt} \\
\mathbf{a}' &= \frac{d^2\mathbf{r}'}{dt^2} \\
&= \frac{d^2R}{dt^2} \cdot \mathbf{r} + 2\frac{dR}{dt} \cdot \frac{d\mathbf{r}}{dt} + R \cdot \frac{d^2\mathbf{r}}{dt^2} \\
&= \frac{d^2R}{dt^2} \cdot R^{-1} \cdot \mathbf{r}' + 2\frac{dR}{dt} \cdot \left(\frac{dR^{-1}}{dt} \cdot \mathbf{r}' + R^{-1} \cdot \frac{d\mathbf{r}'}{dt} \right) + R \cdot \frac{d^2\mathbf{r}}{dt^2} \\
&= -\omega^2\mathbf{r}' - \frac{d\boldsymbol{\Omega}}{dt} \times \mathbf{r}' + 2\omega^2\mathbf{r}' - 2\boldsymbol{\Omega} \times \mathbf{v}' + R \cdot \mathbf{a} \\
&= -\frac{d\boldsymbol{\Omega}}{dt} \times \mathbf{r}' + \omega^2\mathbf{r}' - 2\boldsymbol{\Omega} \times \mathbf{v}' + R \cdot \mathbf{a}
\end{aligned}$$

7.1.3 Specific Angular Momentum

It is often easier to work on specific angular momentum, defined as $\mathbf{H} = \mathbf{r} \times \frac{d\mathbf{r}}{dt}$ (note that both quantities are under K).

For those two primaries and the satellite, $\mathbf{H} = \frac{\mathbf{L}}{m}$ and \mathbf{H} is a constant if and only if \mathbf{L} is a constant. However, it is apparent that the angular momentum \mathbf{L} is fixed for primaries as the mutual gravitational force acting on them is parallel to their displacements. Therefore, for primaries, their \mathbf{H} are constants. Moreover, since for those three objects $\mathbf{H} = \frac{\mathbf{L}}{m}$, we see also that $\omega = \frac{L}{mr^2} = \frac{H}{r^2}$.

For the sake of later discussion, we prove that $\frac{H_{21}}{|\mathbf{r}_2 - \mathbf{r}_1|^2} = \omega$. Let $\mathbf{r}_{21} = \mathbf{r}_2 - \mathbf{r}_1$ and $r_{21} = r_1 + r_2$

$$\begin{aligned}\mathbf{H}_{21} &= (\mathbf{r}_2 - \mathbf{r}_1) \times \left(\frac{d\mathbf{r}_2}{dt} - \frac{d\mathbf{r}_1}{dt} \right) \\ &= \mathbf{r}_2 \times \frac{d\mathbf{r}_2}{dt} - \mathbf{r}_1 \times \frac{d\mathbf{r}_1}{dt} - \mathbf{r}_1 \times \frac{d\mathbf{r}_2}{dt} + \mathbf{r}_1 \times \frac{d\mathbf{r}_1}{dt}\end{aligned}$$

Using the properties of cross product

$$\begin{aligned}H_{21} &= \omega r_1^2 + \omega r_2^2 + r_1 \cdot (|\omega \times \mathbf{r}_2|) + r_2 \cdot (|\omega \times \mathbf{r}_1|) \\ &= \omega \cdot (r_1^2 + r_2^2 + 2r_1 r_2) \\ &= \omega \cdot (r_1 + r_2)^2\end{aligned}$$

Therefore, $\frac{H_{21}}{|\mathbf{r}_2 - \mathbf{r}_1|^2} = \frac{H_{21}}{r_{21}^2} = \omega$

Furthermore, since $\mathbf{r}_1 = -\frac{M_2}{M_1}\mathbf{r}_2$,

$$\begin{aligned}\mathbf{H}_{21} &= (\mathbf{r}_2 - \mathbf{r}_1) \times \left(\frac{d\mathbf{r}_2}{dt} - \frac{d\mathbf{r}_1}{dt} \right) \\ &= \left(1 + \frac{M_2}{M_1} \right)^2 \mathbf{r}_2 \times \left(\frac{d\mathbf{r}_2}{dt} \right) \\ &= \left(1 + \frac{M_2}{M_1} \right)^2 \mathbf{H}_2\end{aligned}$$

Therefore, \mathbf{H}_{21} is a constant like \mathbf{H}_2 and \mathbf{H}_1 .

7.1.4 Implications of Angular-Invariance

In this section, we explore what conclusions can we derive if we know the satellite is angular-invariant for all t . And these conclusions are thus at least necessary but not sufficient for angular-invariant condition, and we can then later use them when solving the equations of motion.

The first conclusion that can be easily derived from the angular-invariant condition is that at any time t , $\frac{r_3}{r_{21}}$ is a constant.

When it is angular-invariant, *at any time* we have to have $\omega_3 = \frac{d\theta}{dt} = \frac{H_{21}}{r_{21}^2}$, which means

$$\frac{H_3}{H_{21}} = \left(\frac{r_3}{r_{21}} \right)^2$$

or ¹

$$\sqrt{\frac{H_3}{H_{21}}} = \frac{r_3}{r_{21}} \quad (1)$$

We now define $\sqrt{\frac{H_3}{H}} = \lambda$ as the fixed ratio $\frac{r_3}{r_{21}}$.

We then want to show that for the satellite to be angular-invariant, the H_3 has to be fixed.

Because under K' r_{21} is horizontal at all the time, when it is angular-invariant, there should be no net tangential force under K' for the satellite. Otherwise, the tangential acceleration will cause the angle between \mathbf{r}_{21}' and \mathbf{r}_3' to change, failing the angular-invariant condition.

If is no net tangential force, the net acceleration is radial for the satellite. Therefore, the Euler's acceleration $-\frac{d\omega}{dt} \times \mathbf{r}_3'$ and the Coriolis acceleration $-2\omega \times \mathbf{v}_3'$ are both perpendicular to the \mathbf{r}_3' and the rest are parallel to \mathbf{r}_3' . We now calculate those two perpendicular forces separately.

Euler's acceleration:

$$\frac{d\omega}{dt} r_3' = \frac{dH_3}{dt} \cdot \frac{H_3}{r_3^3} \cdot \frac{dr_3}{d\theta} - \frac{2H_3^2}{r_3^4} \cdot \frac{dr_3}{d\theta}$$

Coriolis acceleration:

$$2\omega \cdot v_3' = 2 \cdot \frac{H_3^2}{r_3^4} \cdot \frac{dr_3}{d\theta}$$

To cancel out each other, it implies either H_3 is constant, r_3 is constant, or $H_3 = 0$.

Clearly, r_3 and H_3 can both be constant if and only if ω is a constant. However, if ω is not a constant, then r_3 being invariant will contradict with the idea that $\frac{r_3}{r_{21}}$ is invariant, as we all know that in two-body system, the distance between those two primaries are varying with time t . (1)

$H_3 = 0$ means either the satellite has no tangential velocity at all the time, or it always stays at the barycenter. However, having no tangential velocity fails the angular-invariant condition in the first place, unless both primaries have no tangential velocity as well, which is not a solution and should be discarded. Moreover, the force can be easily shown not balanced at the barycenter, therefore, it is impossible for the satellite to always stay at the barycenter. In conclusion, $H_3 = 0$ should be ruled out as reasonable implications of angular-invariance.

Finally, a constant H_3 implies that the net torque $\tau = 0$ for the satellite. This can only be done when the net force under K is parallel to \mathbf{r}_3 . And it further implies that either three bodies are collinear or having some special configuration. This is where we start to construct our equation of motion in the next section.

¹The plus-minus sign is dropped here because both quantities on RHS are positive

7.2 Equations of Motion

7.2.1 Collinear Cases

For the collinear case, we shall only consider the coordinate right to the barycenter O , because the left-hand side solution is equivalent by exchanging the masses of the primaries. Therefore, there are only two regions to discuss: one between O and M_2 , another right to the M_2 according to our definition at 7.1.1.

We now first discuss the first, rightmost region. Given all the above information, one can obtain the following equations of motions for the rightmost elliptical Lagrangian point.

$$\begin{aligned} -\frac{GM_1}{(r_1 + r_2)^2} + \left(\frac{d\theta}{dt}\right)^2 \cdot r_2 &= \frac{d^2 r_2}{dt^2} \\ -\frac{GM_2}{(r_1 + r_2)^2} + \left(\frac{d\theta}{dt}\right)^2 \cdot r_1 &= \frac{d^2 r_1}{dt^2} \\ -\frac{GM_1}{(r_3 + r_1)^2} - \frac{GM_2}{(r_3 - r_2)^2} + \left(\frac{d\theta}{dt}\right)^2 \cdot r_3 &= \frac{d^2 r_3}{dt^2} \end{aligned} \quad (2)$$

Add up the first two equations, and define $r_{21} = r_1 + r_2$, we get the equations reduced to

$$\begin{aligned} -\frac{G(M_1 + M_2)}{r_{21}^2} + \left(\frac{d\theta}{dt}\right)^2 \cdot r_{21} &= \frac{d^2 r_{21}}{dt^2} \\ -\frac{GM_1}{(r_3 + r_1)^2} - \frac{GM_2}{(r_3 - r_2)^2} + \left(\frac{d\theta}{dt}\right)^2 \cdot r_3 &= \frac{d^2 r_3}{dt^2} \end{aligned} \quad (3)$$

It is also easy to know that $r_1 = r_{21} \cdot \frac{M_2}{M_1 + M_2}$ and $r_2 = r_{21} \cdot \frac{M_1}{M_1 + M_2}$.

Now, we want to solve the those two equations of motion. We want to get the solution of r_{21} and r_3 as functions of θ . To do this, we have to eliminate the time derivatives $\frac{d^2 r_{21}}{dt^2}$, $\frac{d^2 r_3}{dt^2}$, $\frac{dr_3}{dt}$, and $\frac{dr_{21}}{dt}$.

$$\begin{aligned} \frac{dr_{21}}{dt} &= \frac{dr_{21}}{d\theta} \frac{d\theta}{dt} \\ &= \frac{dr_{21}}{d\theta} \frac{H_{21}}{r_{21}^2} \end{aligned} \quad (4)$$

Similarly,

$$\frac{dr_3}{dt} = \frac{dr_3}{d\theta} \frac{H_3}{r_3^2} \quad (5)$$

$$\begin{aligned} \frac{d^2 r_{21}}{dt^2} &= \frac{d}{dt} \left(\frac{dr_{21}}{d\theta} \frac{H_{21}}{r_{21}^2} \right) \\ &= \frac{d}{d\theta} \left(\frac{dr_{21}}{d\theta} \frac{H_{21}}{r_{21}^2} \right) \cdot \frac{d\theta}{dt} \\ &= \frac{d}{d\theta} \left(\frac{dr_{21}}{d\theta} \frac{H_{21}}{r_{21}^2} \right) \cdot \frac{H_{21}}{r_{21}^2} \\ &= \frac{d^2 r_{21}}{d\theta^2} \cdot \frac{H_{21}^2}{r_{21}^4} - \left(\frac{dr_{21}}{d\theta} \right)^2 \cdot \frac{2H_{21}^2}{r_{21}^5} \end{aligned} \quad (6)$$

Similarly,

$$\frac{d^2 r_3}{dt^2} = \frac{d^2 r_3}{d\theta^2} \cdot \frac{H_3^2}{r_3^4} - \left(\frac{dr_3}{d\theta}\right)^2 \cdot \frac{2H_3^2}{r_3^5} \quad (7)$$

Using the ratio λ (1), we then define

$$\begin{aligned} \alpha &= G(M_1 + M_2) \\ \beta &= \frac{GM_1}{(1 + \lambda \frac{M_2}{M_1 + M_2})^2} + \frac{GM_2}{(1 - \lambda \frac{M_1}{M_1 + M_2})^2} \end{aligned} \quad (8)$$

Using α, β , and elimination results above (4, 5, 6, 7) about time derivatives, the equation can be rewritten as

$$\begin{aligned} -\frac{\alpha}{r_{21}^2} &= \frac{H_{21}^2}{r_{21}^4} \left(\frac{d^2 r_{21}}{d\theta^2} - \frac{2 \cdot \left(\frac{dr_{21}}{d\theta}\right)^2}{r_{21}} - r_{21} \right) \\ -\frac{\beta}{r_3^2} &= \frac{H_3^2}{r_3^4} \left(\frac{d^2 r_3}{d\theta^2} - \frac{2 \cdot \left(\frac{dr_3}{d\theta}\right)^2}{r_3} - r_3 \right) \end{aligned} \quad (9)$$

Using substitution $r_3 = \frac{1}{s_3}$, and $r_{21} = \frac{1}{s_{21}}$ in the equation 9, one can obtain a set of second order in-homogeneous differential equations

$$\begin{aligned} \frac{\alpha}{H_{21}^2} &= \frac{d^2 s_{21}}{d\theta^2} + s_{21} \\ \frac{\beta}{H_3^2} &= \frac{d^2 s_3}{d\theta^2} + s_3 \end{aligned}$$

Notice that both equations have very similar structures, therefore, it is convenient to study one of them first.

For the first equation, let $s_{21} = e^{k\theta}$, the solution to the homogeneous equation is then $k = \pm i$ where $i = \sqrt{-1}$. And the particular solution of it is a constant $\frac{\alpha}{H_{21}^2}$.

Therefore, the whole solution space of the first equation is then expressed as,

$$s_{21}(\theta) = \frac{\alpha}{H^2} + (A + B) \cos \theta + (A - B)i \sin \theta$$

where A and B are constant, given by $s_{21}(0)$ and $\left.\frac{ds_{21}}{d\theta}\right|_0$.

Fitting in the boundary conditions,

$$\begin{aligned} s_{21}(\theta) &= \frac{\alpha}{H_{21}^2} + \left(s_{21}(0) - \frac{\alpha}{H_{21}^2} \right) \cdot \cos \theta + \left. \frac{ds_{21}}{d\theta} \right|_0 \cdot \sin \theta \\ &= \frac{\alpha}{H_{21}^2} + \sqrt{\left(s_{21}(0) - \frac{\alpha}{H_{21}^2} \right)^2 + \left(\left. \frac{ds_{21}}{d\theta} \right|_0 \right)^2} \cdot \cos(\theta + \phi_{21}) \end{aligned}$$

where

$$\tan \phi_{21} = -\frac{\left. \frac{ds_{21}}{d\theta} \right|_0}{s_{21}(0) - \frac{\alpha}{H_{21}^2}}$$

And we can obtain further that

$$s_{21}(\theta) = \frac{\alpha}{H_{21}^2} (1 + e_{21} \cdot \cos(\theta + \phi_{21}))$$

$$r_{21}(\theta) = \frac{H_{21}^2}{\alpha} \cdot \frac{1}{1 + e_{21} \cdot \cos(\theta + \phi_{21})}$$

where

$$e_{21} = \frac{\sqrt{\left(s_{21}(0) - \frac{\alpha}{H_{21}^2}\right)^2 + \left(\left.\frac{ds_{21}}{d\theta}\right|_0\right)^2}}{\frac{\alpha}{H_{21}^2}}$$

Similar results on r_3 can be obtained using the same methods.

$$r_{21}(\theta) = \frac{H_{21}^2}{\alpha} \cdot \frac{1}{1 + e_{21} \cdot \cos(\theta + \phi_{21})}$$

$$r_3(\theta) = \frac{H_3^2}{\beta} \cdot \frac{1}{1 + e_3 \cdot \cos(\theta + \phi_3)}$$

Since both equations are equations of ellipse in polar coordinate, $\frac{r_3}{r_{21}}$ then further implies that those two ellipses are similar, and thus e_3 has to be the same as e_{21} . And that further implies that $\phi_{21} = \phi_3$, otherwise $\frac{1+e_3 \cdot \cos(\theta+\phi_{21})}{1+e_3 \cdot \cos(\theta+\phi_3)}$ cannot be constant under all θ .

Using those two equations and the constraint ratio λ ,

$$\sqrt{\frac{H_3}{H_{21}}} = \frac{r_3}{r_{21}} = \left(\frac{H_3}{H_{21}}\right)^2 \cdot \frac{\alpha}{\beta}$$

we have

$$\frac{\beta}{\alpha} = \left(\frac{H_3}{H_{21}}\right)^{\frac{3}{2}}$$

$$\lambda = \frac{r_3}{r_{21}} = \left(\frac{\beta}{\alpha}\right)^{\frac{1}{3}}$$

Finally, we can obtain the λ using the following equation according to equation 8,

$$\lambda^3(M_1 + M_2) = \frac{M_1}{\left(1 + \frac{M_2}{\lambda \cdot (M_1 + M_2)}\right)^2} + \frac{M_2}{\left(1 - \frac{M_1}{\lambda \cdot (M_1 + M_2)}\right)^2}$$

Let $\mu = \frac{M_2}{M_1 + M_2}$. The above expression can be simplified as

$$\lambda^3 = \frac{1 - \mu}{\left(1 + \frac{\mu}{\lambda}\right)^2} + \frac{\mu}{\left(1 - \frac{1-\mu}{\lambda}\right)^2}$$

By changing the sign of gravitational forces in equation 2, one can also calculate other different points. For the point between O and M_2 :

$$\lambda^3 = \frac{1 - \mu}{(1 + \frac{\mu}{\lambda})^2} - \frac{\mu}{(1 - \frac{1-\mu}{\lambda})^2}$$

For points left to the origin O , they are essentially the same as the right-hand side case, except with mass exchanged. i.e. $\mu' = 1 - \mu$.

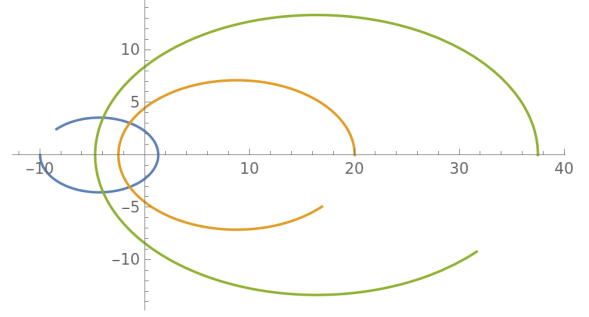


Figure 3: The orbit of a particular collinear solution.

7.2.2 Non-collinear Cases

For non-collinear cases, primaries and satellite form a triangle with edges $\mathbf{r}_2 - \mathbf{r}_1$, $\mathbf{r}_3 - \mathbf{r}_2$, and $\mathbf{r}_3 - \mathbf{r}_1$. Let the angle that $\mathbf{r}_3 - \mathbf{r}_1$ makes with $\mathbf{r}_2 - \mathbf{r}_1$ be ϕ .

The general equation of motion of the satellite is then

$$-\frac{GM_1}{|\mathbf{r}_3 - \mathbf{r}_1|^3} \cdot (\mathbf{r}_3 - \mathbf{r}_1) - \frac{GM_2}{|\mathbf{r}_3 - \mathbf{r}_2|^3} \cdot (\mathbf{r}_3 - \mathbf{r}_2) + \omega^2 \cdot \mathbf{r}_3 = \frac{d^2 \mathbf{r}_3}{dt^2} \quad (10)$$

Since we have to ensure that there is no net torque, we then have to make sure

$$\frac{GM_1}{|\mathbf{r}_3 - \mathbf{r}_1|^3} \cdot \mathbf{r}_1 = -\frac{GM_2}{|\mathbf{r}_3 - \mathbf{r}_2|^3} \cdot \mathbf{r}_2$$

Since $\mathbf{r}_1 = -\frac{M_2}{M_1} \mathbf{r}_2$, above condition is equivalent to

$$|\mathbf{r}_3 - \mathbf{r}_1|^3 = |\mathbf{r}_3 - \mathbf{r}_2|^3$$

We thus define $|\mathbf{r}_3 - \mathbf{r}_1|^3 = |\mathbf{r}_3 - \mathbf{r}_2|^3 = d^3$. That implies the triangle is an isosceles. Because it is now all the vector quantities are parallel, we take the magnitudes of these quantities, and the equation of motion then becomes

$$-\frac{G(M_1 + M_2)}{d^3} \cdot r_3 + \omega^2 \cdot r_3 = \frac{d^2 r_3}{dt^2}$$

Since we know that this is isosceles, the x coordinate of \mathbf{r}_3 is then determined as $\frac{r_{21}}{2} - \mu r_{21}$.

Using ϕ , $\mathbf{r}_3 = \left(\frac{r_{21}}{2} - \mu r_{21}, \frac{r_{21} \cdot \tan \phi}{2} \right)$ and $d = \frac{r_{21}}{2 \cos \phi}$, the equation of motion can further be

$$-\frac{G(M_1 + M_2) \cdot 8 \lambda^3 \cos^3 \phi}{r_3^2} + \omega^2 \cdot r_3 = \frac{d^2 r_3}{dt^2}$$

Notice this equation is in the same form as the collinear case in equation 3. Therefore, in these cases, β becomes $G(M_1 + M_2) \cdot 8 \lambda^3 \cos^3 \phi$. Since $\lambda^3 \cdot \alpha = \beta$, it finally reduces to

$$\cos \phi = \frac{1}{2}$$

This tells us that the triangle is equilateral, and it could be either in first quadrant or fourth quadrant.

8 Stability Analysis

Without declaring explicitly, all the quantities in this section are assumed to be relative to K' .

8.1 General Analysis

Let $r = r_{21}$. At any given coordinate $\begin{pmatrix} x \\ y \end{pmatrix}$, the acceleration exerted on the satellite is given by

$$\begin{pmatrix} \ddot{x} \\ \ddot{y} \end{pmatrix} = -\frac{GM_1}{d_1^3} \begin{pmatrix} x + \mu r \\ y \end{pmatrix} - \frac{GM_2}{d_2^3} \begin{pmatrix} x - (1 - \mu)r \\ y \end{pmatrix} + \omega^2 \begin{pmatrix} x \\ y \end{pmatrix} - 2\omega \begin{pmatrix} -y \\ x \end{pmatrix} - \frac{d\omega}{dt} \begin{pmatrix} -y \\ x \end{pmatrix} \quad (11)$$

where $\mu = \frac{M_2}{M_1 + M_2}$

In order to obtain a linear approximation, for the first and the second term, we then use component-wise Taylor expansion at a fixed point $\begin{pmatrix} x_0 \\ y_0 \end{pmatrix}$.

$$\begin{aligned} -\frac{GM_1}{d_1^3} \cdot (x + \mu r) &\approx -GM_1 \left[\frac{x_0 + \mu r}{[(x_0 + \mu r)^2 + y_0^2]^{3/2}} + \frac{\partial}{\partial x} \left(\frac{x + \mu r}{d_1^3} \right) \Big|_{(x_0, y_0)} (x - x_0) \right. \\ &\quad \left. + \frac{\partial}{\partial y} \left(\frac{x + \mu r}{d_1^3} \right) \Big|_{(x_0, y_0)} (y - y_0) \right] \\ &= -GM_1 \left[\frac{x_0 + \mu r}{[(x_0 + \mu r)^2 + y_0^2]^{3/2}} + \frac{d_1^3 - (x + \mu r) \cdot 3d_1^2 \cdot \frac{\partial d_1}{\partial x}}{d_1^6} \Big|_{(x_0, y_0)} (x - x_0) \right. \\ &\quad \left. + \frac{-(x + \mu r) \cdot 3d_1^2 \cdot \frac{\partial d_1}{\partial y}}{d_1^6} \Big|_{(x_0, y_0)} (y - y_0) \right] \\ &= -GM_1 \left[\frac{x_0 + \mu r}{[(x_0 + \mu r)^2 + y_0^2]^{3/2}} + \left(\frac{1}{d_1^3|_{(x_0, y_0)}} \right. \right. \\ &\quad \left. \left. - \frac{3(x_0 + \mu r)^2}{d_1^5|_{(x_0, y_0)}} \right) (x - x_0) - \frac{3(x_0 + \mu r)y_0}{d_1^5|_{(x_0, y_0)}} (y - y_0) \right] \end{aligned} \quad (12)$$

Similarly,

$$\begin{aligned}
-\frac{GM_1}{d_1^3}y &\approx -GM_1 \left[\frac{y_0}{[(x_0 + \mu r)^2 + y_0^2]^{3/2}} - \frac{3y_0(x_0 + \mu r)}{d_1^5|_{(x_0, y_0)}}(x - x_0) + \frac{3y_0^2}{d_1^5|_{(x_0, y_0)}}(y - y_0) \right] \\
-\frac{GM_2}{d_2^3}(x - (1 - \mu)r) &\approx -GM_1 \left[\frac{x_0 - (1 - \mu)r}{[(x_0 - (1 - \mu)r)^2 + y_0^2]^{3/2}} + \left(\frac{1}{d_1^3|_{(x_0, y_0)}} - \frac{3(x_0 - (1 - \mu)r)^2}{d_1^5|_{(x_0, y_0)}} \right)(x - x_0) \right. \\
&\quad \left. - \frac{3(x_0 - (1 - \mu)r)y_0}{d_1^5|_{(x_0, y_0)}}(y - y_0) \right] \\
-\frac{GM_2}{d_2^3}y &\approx -GM_2 \left[\frac{y_0}{[(x_0 - (1 - \mu)r)^2 + y_0^2]^{3/2}} - \frac{3y_0(x_0 - (1 - \mu)r)}{d_2^5|_{(x_0, y_0)}}(x - x_0) \right. \\
&\quad \left. - \frac{3y_0^2}{d_2^5|_{(x_0, y_0)}}(y - y_0) \right]
\end{aligned}$$

We now introduce infinitesimal perturbation into the system, let $\begin{pmatrix} x_0 \\ y_0 \end{pmatrix}$ be one elliptical lagrange point, we take

$$\begin{pmatrix} x' \\ y' \end{pmatrix} = \begin{pmatrix} x_0 \\ y_0 \end{pmatrix} + \begin{pmatrix} \delta x \\ \delta y \end{pmatrix}$$

We then have

$$\begin{aligned}
\delta \dot{x} &= \frac{dx'}{dt} - \frac{dx_0}{dt} \\
&= \frac{d\delta x}{dt} \\
\delta \ddot{x} &= \frac{d}{dt} \left(\frac{dx'}{dt} \right) - \frac{d^2 x_0}{dt^2} \\
&= \frac{d^2 x_0}{dt^2} + \frac{d^2 \delta x}{dt^2} - \frac{d^2 x_0}{dt^2} \\
&= \frac{d}{dt} \delta \dot{x}
\end{aligned}$$

Finally, we can obtain a linear system. Thus, we can write out an equation relating $\delta x, \delta y, \delta \dot{x}, \delta \dot{y}$ using matrix notation.

$$\frac{d}{dt} \begin{pmatrix} \delta x \\ \delta y \\ \delta \dot{x} \\ \delta \dot{y} \end{pmatrix} = \begin{pmatrix} 0 & 0 & 1 & 0 \\ 0 & 0 & 0 & 1 \\ -U_{xx}^G + \omega^2 & -U_{xy}^G + \frac{d\omega}{dt} & 0 & 2\omega \\ -U_{xy}^G - \frac{d\omega}{dt} & -U_{yy}^G + \omega^2 & -2\omega & 0 \end{pmatrix} \begin{pmatrix} \delta x \\ \delta y \\ \delta \dot{x} \\ \delta \dot{y} \end{pmatrix} \quad (13)$$

where notations like U_{xx}^G is the second order partial derivative of the gravitational potential in x direction, or the negative first order partial derivative of gravitational acceleration in x direction.

8.2 Analysis on Stability of Non-collinear Circular Cases

Under circular circumstances, $\frac{d\omega}{dt} = 0$, $\frac{G(M_1+M_2)}{r^3} = \omega^2$, and r_{21} is a constant.

Evaluating at $\begin{pmatrix} \frac{r_{21}}{2}(1-2\mu) \\ \frac{\sqrt{3}}{2}r_{21} \end{pmatrix}$, we thus obtain the matrix

$$\begin{pmatrix} 0 & 0 & 1 & 0 \\ 0 & 0 & 0 & 1 \\ \frac{3}{4}\omega^2 & \frac{3\sqrt{3}}{4}(1-2\mu)\omega^2 & 0 & 2\omega \\ \frac{3\sqrt{3}}{4}(1-2\mu)\omega^2 & \frac{9}{4}\omega^2 & -2\omega & 0 \end{pmatrix}$$

The matrix has four eigenvalues

$$\pm \frac{\omega}{2} \sqrt{2 \pm \sqrt{27(1-2\mu)^2 - 23}} i$$

In order to ensure four eigenvalues being purely imaginary, we have to ensure

$$\sqrt{2 \pm \sqrt{27(1-2\mu)^2 - 23}}$$

is real.

However, $(1-2\mu)^2 < 1$ as $-1 < \mu < 1$, and $27(1-2\mu)^2 - 23 < 2$. Therefore, the only thing to ensure is that

$$27(1-2\mu)^2 - 23 \geq 0$$

which gives us

$$1 - \sqrt{\frac{23}{27}} \geq 2\mu$$

or

$$1 + \sqrt{\frac{23}{27}} \leq 2\mu$$

Notice they are congruent, therefore, it is enough to consider one of them. Therefore, the stable condition becomes

$$\frac{M_1}{M_2} \geq \frac{1 + \sqrt{\frac{23}{27}}}{1 - \sqrt{\frac{23}{27}}}$$

8.3 Stability of Non-collinear cases through Simulation

To determine the stability of the non-collinear cases (L4, L5), a simulation was built to model the motion predicted in the sections above.

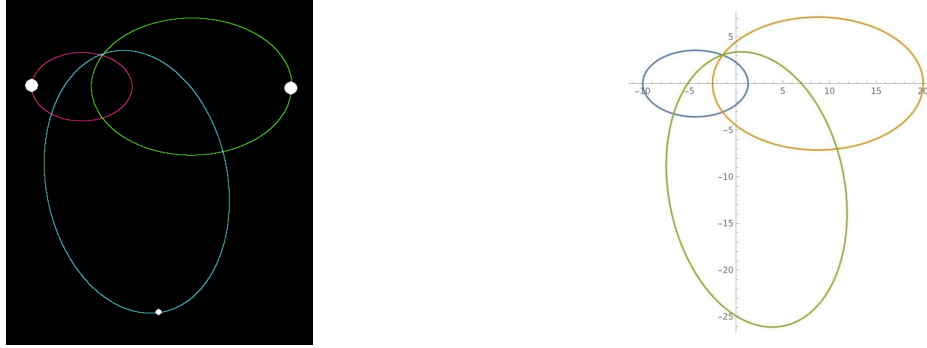
8.3.1 Construction of the Model

The simulation was built using an iterative method to solve the initial value problem with

1. The ODE generated by Newton's Second Law,
2. The initial conditions as predicted by our theoretical work from the previous sections.

The full program is included in Appendix [A](#).

In order to determine the accuracy of the simulation, a trial run was done with initial conditions without perturbation and the result was compared to the theoretical prediction. The comparison is visualized in Figure 4.



(a) Results from the iterative simulation.

(b) Original solution of a non-collinear case.

Figure 4: Comparison between the original result and the simulated result.

From the figure, we can see that the two orbits do fit in shape. The three bodies remained on the vertices of an equilateral triangle throughout the orbit, and this did fit with the original objective to find the angular-invariant solutions of the three-body problem. The three orbits were individual ellipses, and it seems that this is a good solution to the elliptical restricted three-body problem.

However, it is clear that the three bodies did not return to the exact initial positions after one full period, and the authors predict that this originates from the iterative nature of the simulation. Since the ODEs were solved through Euler's method, the deviation should increase with the time step taken. This hypothesis is verified by running the simulation for the same initial conditions and different time steps. The gap between periods did decrease with smaller time steps and the orbits approximated perfect ellipses. This effect from the nature of the simulation will be treated as a systematic error and taken into account in further analysis and evaluation.

8.3.2 Effect of Perturbations

The impact of perturbations on the orbits is analyzed by changing the initial speeds of the satellite by a certain percentage. Eight different runs were done with percentage changes ranging from 0.1% to 1.0%. The results are shown in Figure 5.

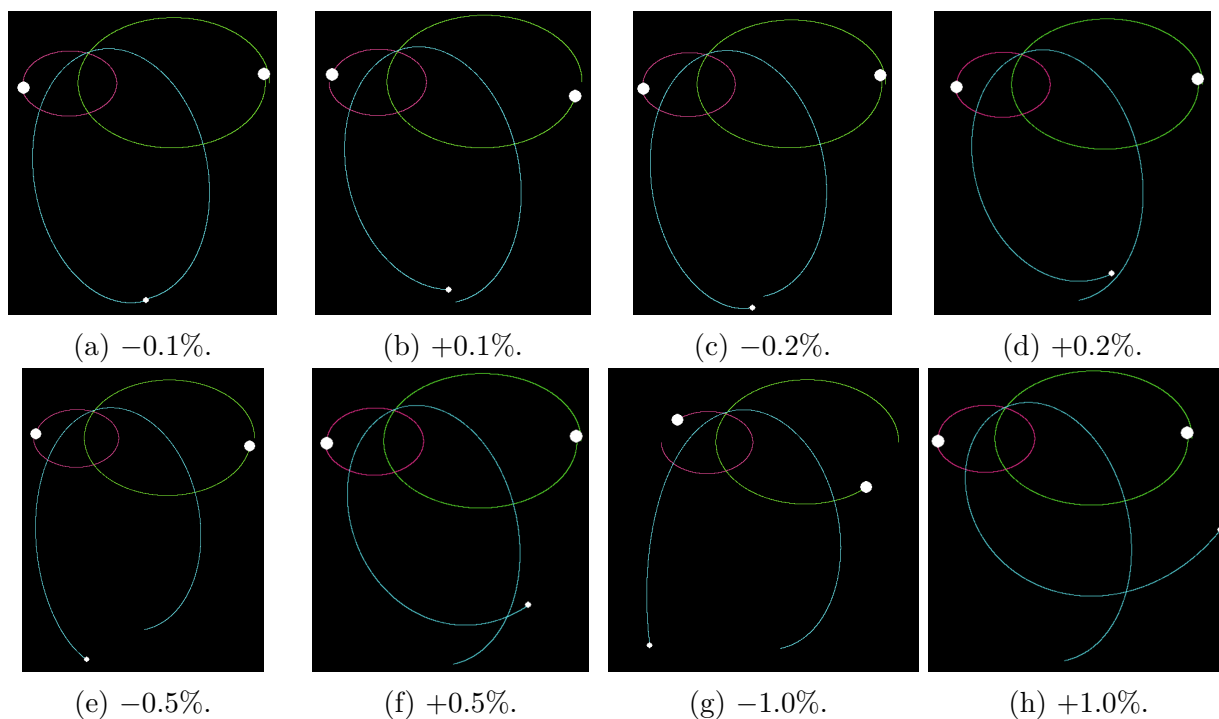


Figure 5: Orbits when the initial speed is changed by a certain percentage.

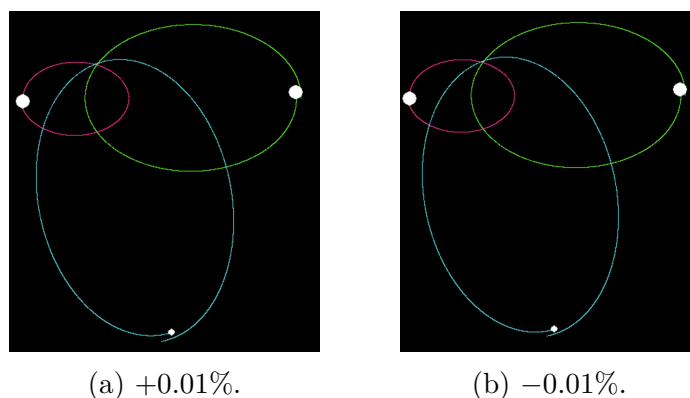
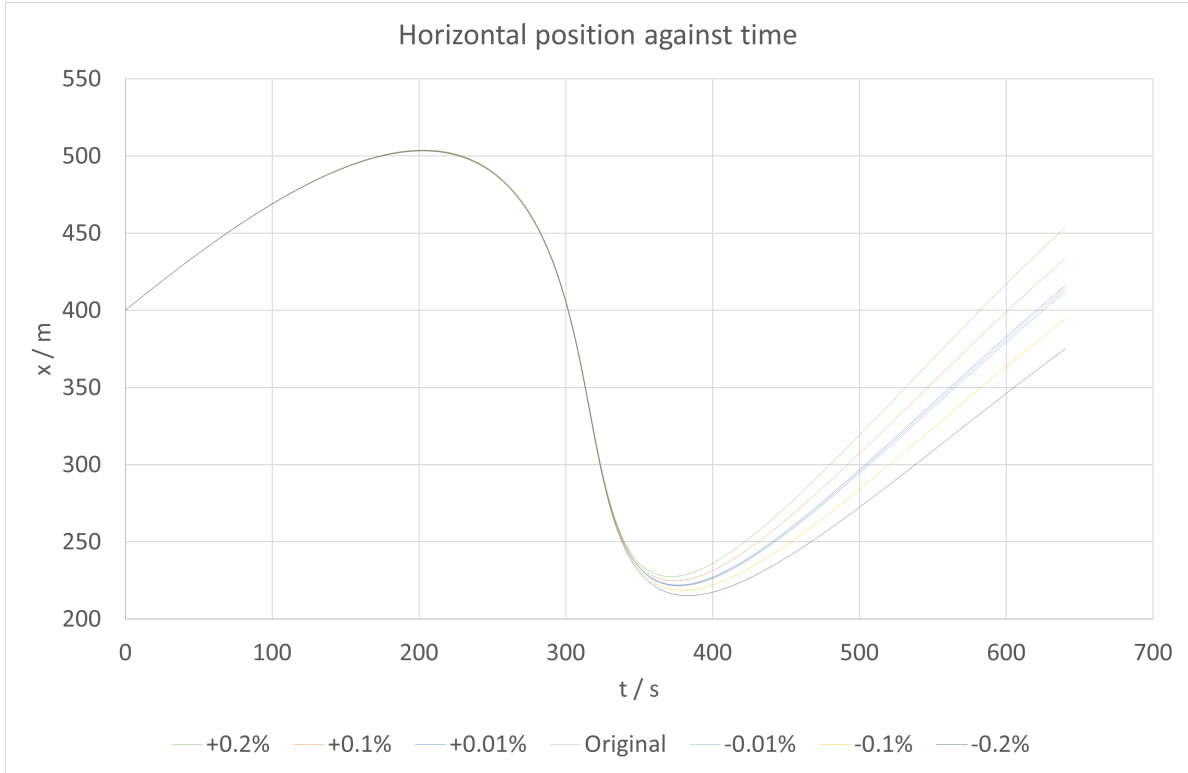
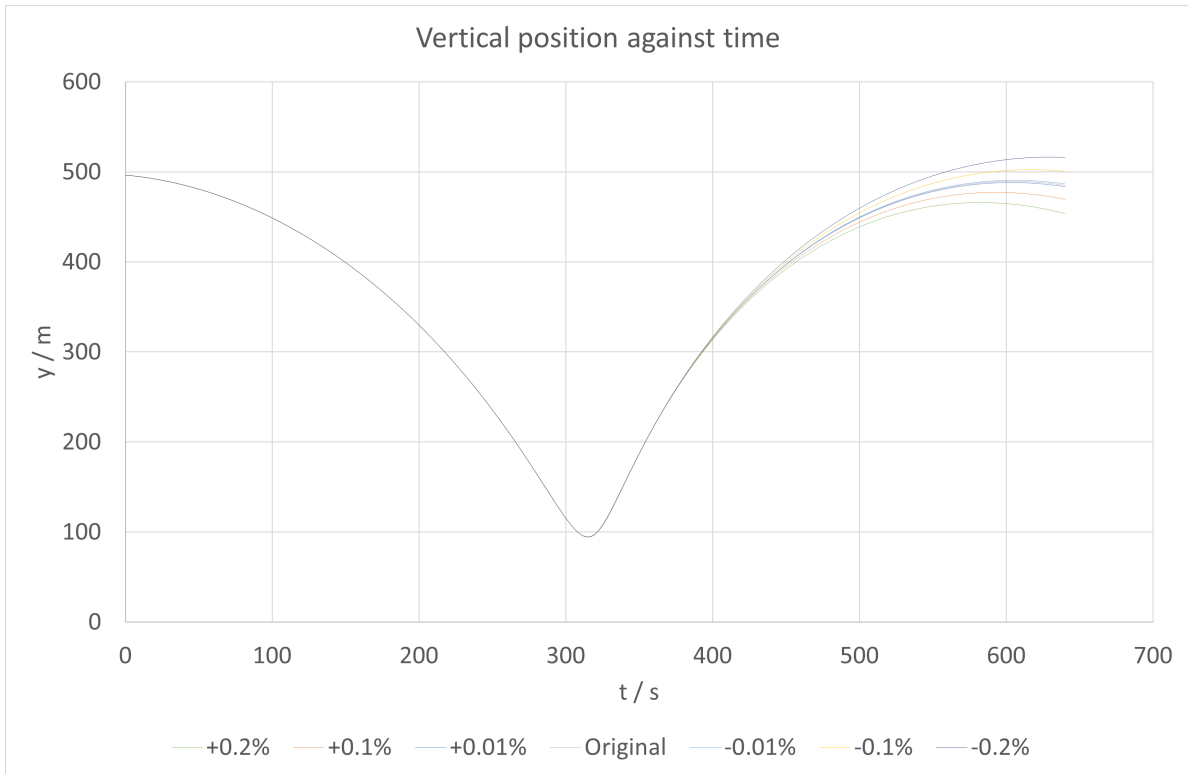


Figure 6: Two more runs for smaller deviations in speed.



(a) Horizontal position against time.



(b) Vertical position against time.

Figure 7: Plots of position against time.

By comparing Figures 5a, 5c, 5e and 5g, we can see that an incremental decrease in initial velocity results in the escape of the satellite from the system after one period. On the contrary, Figures 5b, 5d, 5f and 5h show that increasing the initial velocity results in the satellite falling into a lower orbit relative to the two primaries. This is counter-intuitive, as we would expect to see satellites with higher velocity (more kinetic energy) to escape easily.

Also, Figures 5a and 5b show that for changes of velocity within $\pm 0.1\%$ of the theoretical velocity, the satellite still moves in an elliptical orbit within the range of systematic error as compared to 4a. However, Figures 5c and 5d generate results that are out of error range and therefore suggest that a $\pm 0.2\%$ would cause the system to destabilize.

To verify this observation, two additional runs were made for smaller perturbations Figure 6. The changes of the speeds were $\pm 0.01\%$ respectively.

These two figures confirm that within the range of $< \pm 0.1\%$, the satellite does orbit in a near-elliptical orbit.

The x and y positions of the satellites were plotted against time for $\pm 0.2\%$, $\pm 0.1\%$ and $\pm 0.01\%$, as shown in Figure 7.

Even though these graphs do not show the clear boundary between the $\pm 0.2\%$ and $\pm 0.1\%$ runs, it does confirm that the deviation from the original orbit increases with the change in speed.

From the analysis above, we can conclude that the maximum stable range for the satellite to operate in a restricted angular-invariant orbit is between $\pm 0.1\%$ and $\pm 0.2\%$.

Simulations for speed deviations over $\pm 1.0\%$ were also done, and this resulted in chaotic three-body behaviour. Since this is not directly related to the stability of our desired cases, the corresponding graphs are presented in Appendix B.

Part IV

Conclusion

9 Solutions to the Problem

Our research shows the existence and the solutions to the elliptical restricted three-body problem in a Lagrangian setup. The solution constraint provided can be directly reduced back to the circular Lagrange points since the ratios are not dependent on initial conditions other than masses. Moreover, the nonlinear solutions to the problem are found to be in the same condition as that of the circular one.

10 Stability of the Solutions

From our research, we used an iterative simulation to predict the stability of our solutions. We found that the elliptical orbits of the satellites were stable for initial speeds within $\pm 0.1\%$ of the calculated optimal speed. For speeds over $\pm 1.0\%$ from the optimal, chaotic behavior is predicted and orbits are destructive, either escaping the system or crashing into the primaries.

Works Cited

- Broucke, R. “Stability of periodic orbits in the elliptic, restricted three-body problem.” *AIAA Journal*, vol. 7, no. 6, 1969, _eprint: <https://doi.org/10.2514/3.5267>, pp. 1003–1009. doi:[10.2514/3.5267](https://doi.org/10.2514/3.5267).
- Cruz, João. “Stability of Circular Orbits in the Three Body Problem”. 2020. Instituto Superior Técnico, Universidade de Lisboa, MSc thesis.
- Montgomery, Richard and Alain Chenciner. “A Remarkable Periodic Solution of the Three-Body Problem in the Case of Equal Masses”. *Annals of mathematics, ISSN 0003-486X, Vol. 152, N^o 3, 2000, pags. 881-901*, vol. 152, 2000. doi:[10.2307/2661357](https://doi.org/10.2307/2661357).
- Sussman, Gerald Jay and Jack Wisdom. “Numerical Evidence that the Motion of Pluto is Chaotic”. *Science*, vol. 241, no. 4864, 22 July 1988, pp. 433–437. *JSTOR*, www.jstor.org/stable/1701411. Accessed 28 Mar. 2021.

Appendix

A Programs

Code 1: Iterative program for stability analysis.

```
1 import pygame, sys, random, math
2
3 def draw(scr, x1, y1, x2, y2, x3, y3):
4     global pointList1, pointList2
5     for i in range(2, len(pointList1)):
6         point1 = pointList1[i]
7         point2 = pointList1[i - 1]
8         pygame.draw.line(scr, (255, 51, 153), point1,\
9                          point2, 1)
10    for i in range(2, len(pointList2)):
11        point1 = pointList2[i]
12        point2 = pointList2[i - 1]
13        pygame.draw.line(scr, (102, 255, 51), point1,\
14                          point2, 1)
15    for i in range(2, len(pointList3)):
16        point1 = pointList3[i]
17        point2 = pointList3[i - 1]
18        pygame.draw.line(scr, (97, 238, 245), point1,\
19                          point2, 1)
20    pygame.draw.circle(scr, (255, 255, 255), (x1, y1), 10, 0)
21    pygame.draw.circle(scr, (255, 255, 255), (x2, y2), 10, 0)
22    pygame.draw.circle(scr, (255, 255, 255), (x3, y3), 5, 0)
23
24 def move1():
25     global x1, y1, vx1, vy1, x2, y2, G, m1, m2, dt
26     dx, dy = x1 - x2, y1 - y2
27     r = (dx * dx + dy * dy) ** 0.5
28     a1 = G * m2 / r / r
29     ax1 = -a1 * dx / r
30     ay1 = -a1 * dy / r
31     vx1 += ax1 * dt
32     vy1 += ay1 * dt
33     x1 += vx1 * dt
34     y1 += vy1 * dt
35     pointList1.append((x1, y1))
36
37 def move2():
38     global x1, y1, vx2, vy2, x2, y2, G, m1, m2, dt
39     dx, dy = x2 - x1, y2 - y1
40     r = (dx * dx + dy * dy) ** 0.5
41     a2 = G * m1 / r / r
42     ax2 = -a2 * dx / r
43     ay2 = -a2 * dy / r
44     vx2 += ax2 * dt
45     vy2 += ay2 * dt
46     x2 += vx2 * dt
47     y2 += vy2 * dt
48     pointList2.append((x2, y2))
49
50 def move3():
51     global x1, y1, vx3, vy3, x2, y2, G, m1, m2, dt, x3, y3
52     dx1, dy1 = x3 - x1, y3 - y1
53     r = (dx1 * dx1 + dy1 * dy1) ** 0.5
54     a31 = G * m1 / r / r
55     ax31 = -a31 * dx1 / r
56     ay31 = -a31 * dy1 / r
57     dx2, dy2 = x3 - x2, y3 - y2
58     r = (dx2 * dx2 + dy2 * dy2) ** 0.5
```

```

59     a32 = G * m2 / r / r
60     ax32 = -a32 * dx2 / r
61     ay32 = -a32 * dy2 / r
62     ax3 = ax31+ax32
63     ay3 = ay31+ay32
64     vx3 += ax3 * dt
65     vy3 += ay3 * dt
66     x3 += vx3 * dt
67     y3 += vy3 * dt
68     pointList3.append((x3, y3))
69
70 #screen init
71 SCREEN_W, SCREEN_H = 800, 600
72
73 #data set
74 x1, y1 = 200, 150
75 x2, y2 = 600, 150
76 vx1, vy1 = 0, 0.3
77 vx2, vy2 = 0, -0.6
78 m1 = 2
79 m2 = 1
80
81 #perturbation
82 k = 0.9999
83
84 #satellite
85 x3, y3 = 400, 496.41
86 vx3 = 0.7794228634 * k
87 vy3 = -0.15 * k
88 m3 = 1
89
90 #data init
91 G = 400
92 t = 0
93 dt = 0.1
94 pointList1 = []
95 pointList2 = []
96 pointList3 = []
97
98 #pygame init
99 pygame.init()
100 screen = pygame.display.set_mode((SCREEN_W, SCREEN_H))
101 clock = pygame.time.Clock()
102
103
104 #main loop
105 for i in range(6400):
106     for event in pygame.event.get():
107         if event.type == pygame.QUIT:
108             pygame.quit()
109             sys.exit()
110     screen.fill((0, 0, 0))
111     move1()
112     move2()
113     move3()
114     draw(screen, int(x1), int(y1), int(x2), int(y2), int(x3), int(y3))
115     pygame.display.update()
116     clock.tick(100)
117     t += 1
118
119 while True:
120     for event in pygame.event.get():
121         if event.type == pygame.QUIT:
122             pygame.quit()
123             sys.exit()

```

B Graphs

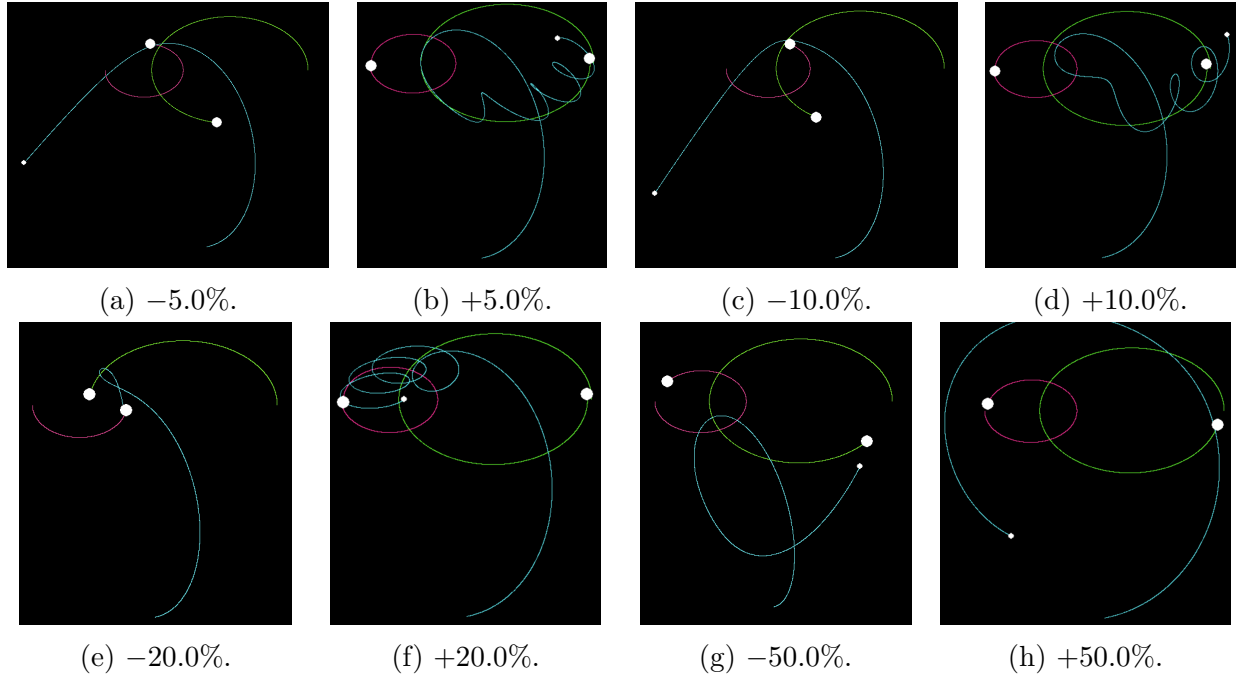


Figure 8: Orbits when the initial speed is changed by a certain percentage.